

# A Lightweight Approach for Reflectance Estimation On-the-Fly

## Supplementary Material

Kihwan Kim<sup>1</sup> Jinwei Gu<sup>1</sup> Stephen Tyree<sup>1</sup> Pavlo Molchanov<sup>1</sup>  
 Matthias Nießner<sup>2</sup> Jan Kautz<sup>1</sup>

<sup>1</sup>NVIDIA <sup>2</sup>Technical University of Munich

<http://research.nvidia.com/publication/reflectance-estimation-fly>



This supplementary material provides further results for the synthetic data evaluation performed in Section 4 of the main paper. In Table 1, we enumerate the RMSE for each of the ten randomly sampled materials in the user study. For a qualitative comparison of each method, Figures 1-3 show the user study renderings (described in Section 4.1) for six of the materials. Finally, Figure 4 shows further examples from Figure 9 in the main paper. Additional visualizations and results are found in the supplementary video located at <http://research.nvidia.com/publication/reflectance-estimation-fly>.

Network	Loss	RMSE										
		Avg	m3331	m3905	m1161	m3522	m3665	m1891	m586	m2646	m3601	m947
Grouplet	$RMSE_1 + E_c$	0.455	0.389	0.224	0.388	0.885	0.658	0.504	0.427	0.112	0.135	0.272
Grouplet	$RMSE_1$	0.432	0.493	0.232	0.235	0.734	0.729	0.514	0.452	0.175	0.119	0.200
HemiCNN	$RMSE_2$	0.564	0.153	0.130	1.341	1.012	0.588	0.480	0.406	0.026	0.184	0.370
HemiCNN	CubeRoot	0.439	0.356	0.095	1.282	0.841	0.680	0.197	0.557	0.233	0.304	0.536
HemiCNN	$RMSE_1$	0.419	0.102	0.080	1.082	0.966	0.630	0.288	0.507	0.075	0.207	0.325
HemiCNN	$CubeRoot + E_c$	0.583	0.481	0.161	1.274	0.878	0.742	0.269	0.590	0.283	0.330	0.454
Grouplet	$RMSE_2$	0.457	0.493	0.232	0.440	0.707	0.665	0.514	0.378	0.058	0.155	0.386

TABLE 1: **Extension of Table 2 from the main paper.** RMSE (w.r.t ground truth BRDF parameters normalized to zero mean and unit variance) on the test set of SynBRDF (Avg) and on the ten randomly sampled test set materials shown to users in the perceptual study (described in Section 4.1).

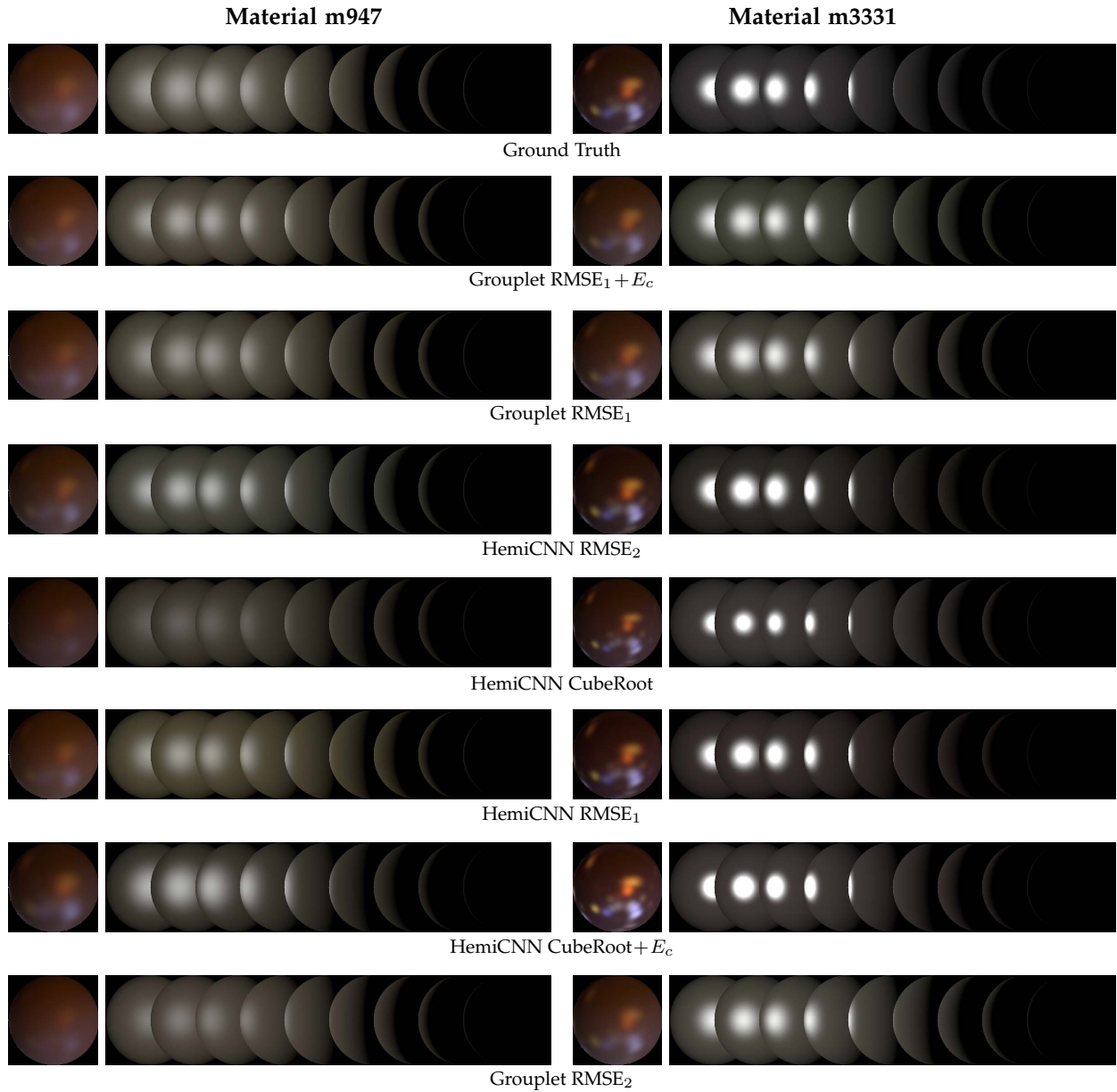


Fig. 1: Qualitative comparison of proposed methods on *m947* (left) and *m3331* (right). For each material, we show a rendered image under natural illumination, as well as under varying light sources. The top row is the ground truth, while the remaining rows depict estimated BRDF from variations of the proposed method. Please refer to the main paper for details of each variation.

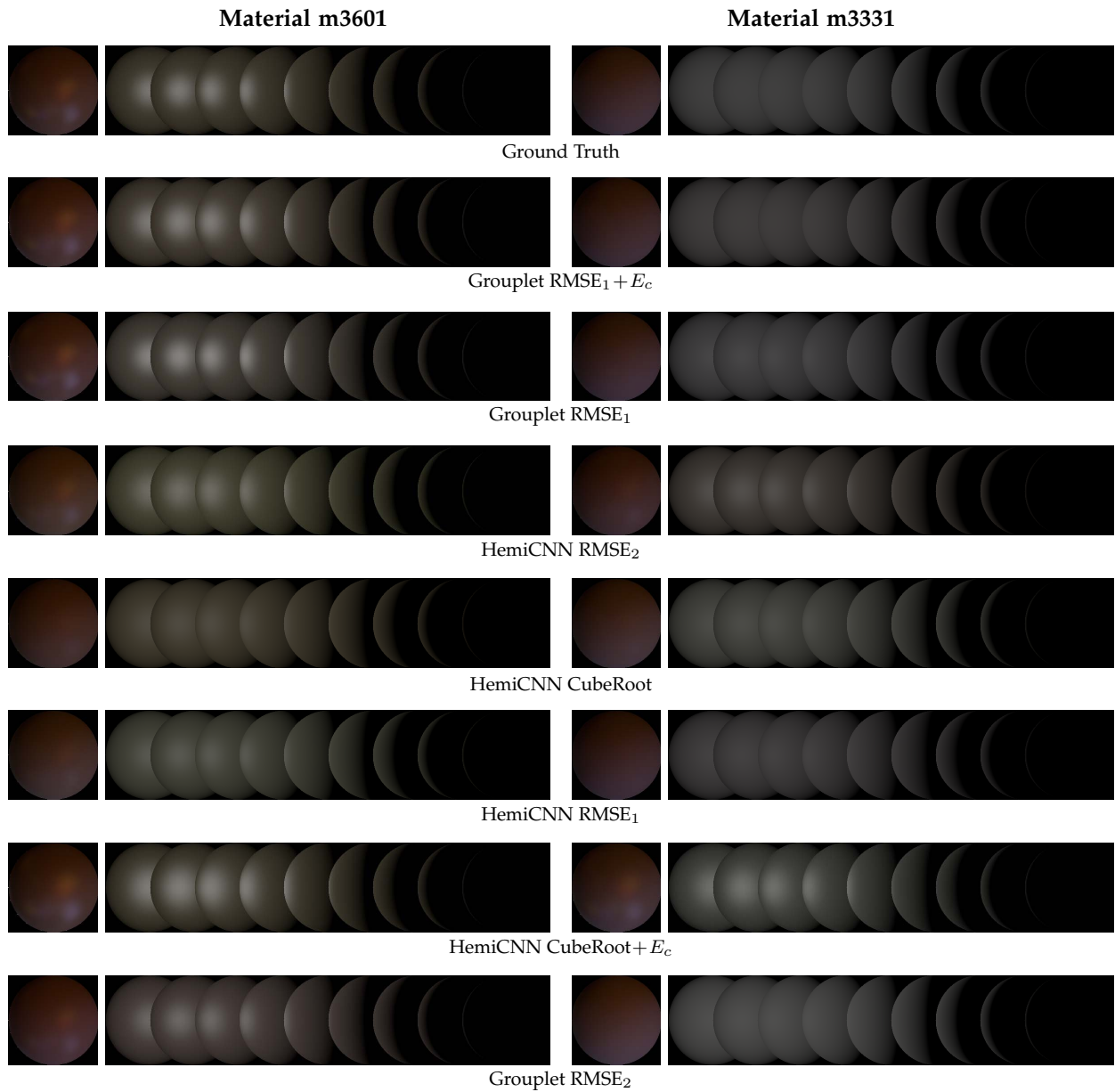


Fig. 2: Qualitative comparison of proposed methods on  $m3601$  (left) and  $m3905$  (right). For each material, we show a rendered image under natural illumination, as well as under varying light sources. The top row is the ground truth, while the remaining rows depict estimated BRDF from variations of the proposed method. Please refer to the main paper for details of each variation.

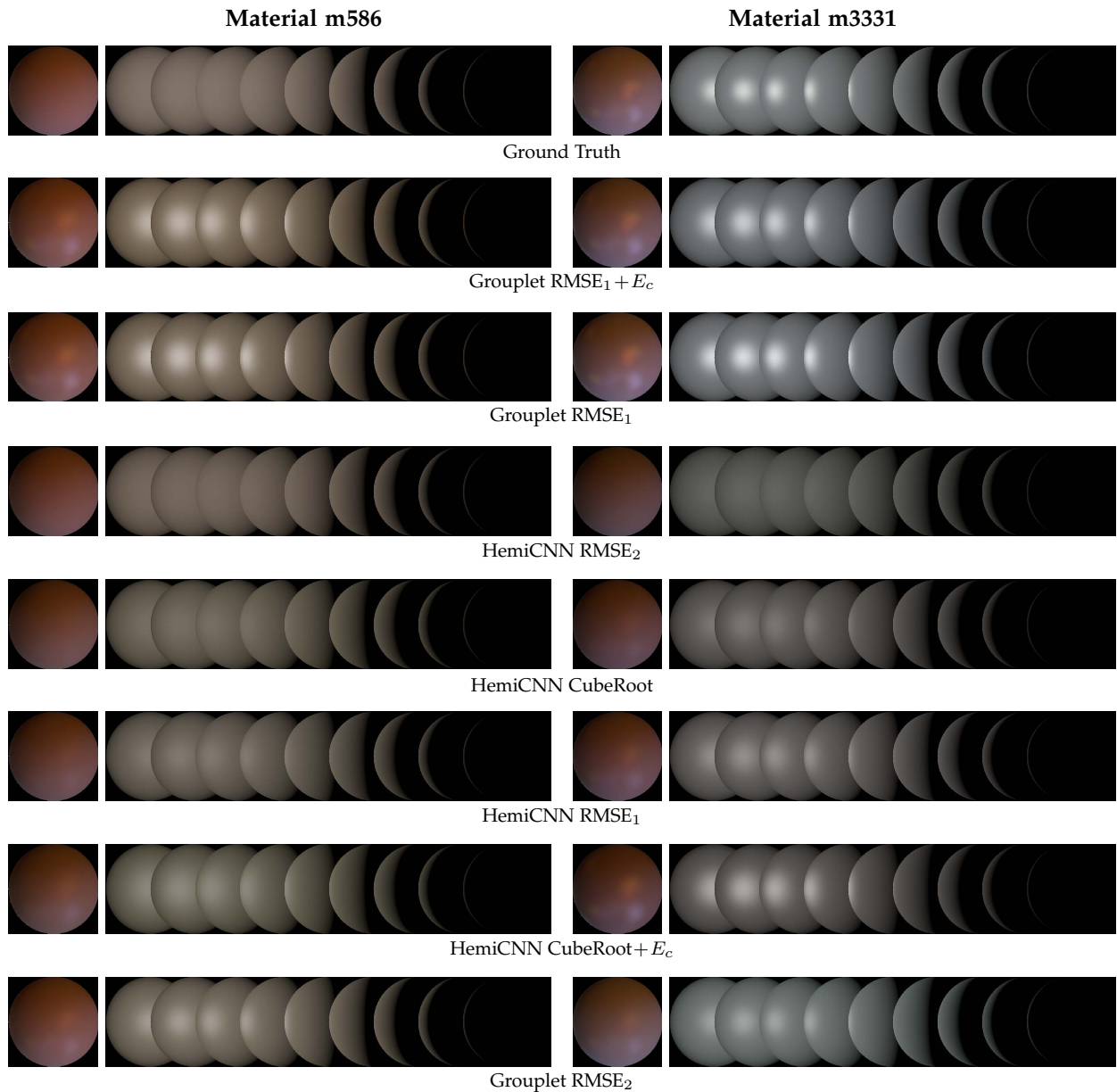


Fig. 3: Qualitative comparison of methods for  $m586$  (left) and  $m1161$  (right). For each material, we show a rendered image under natural illumination, as well as under varying light sources. The top row is the ground truth, while the remaining rows depict estimated BRDF from variations of the proposed method. Please refer to the main paper for details of each variation.

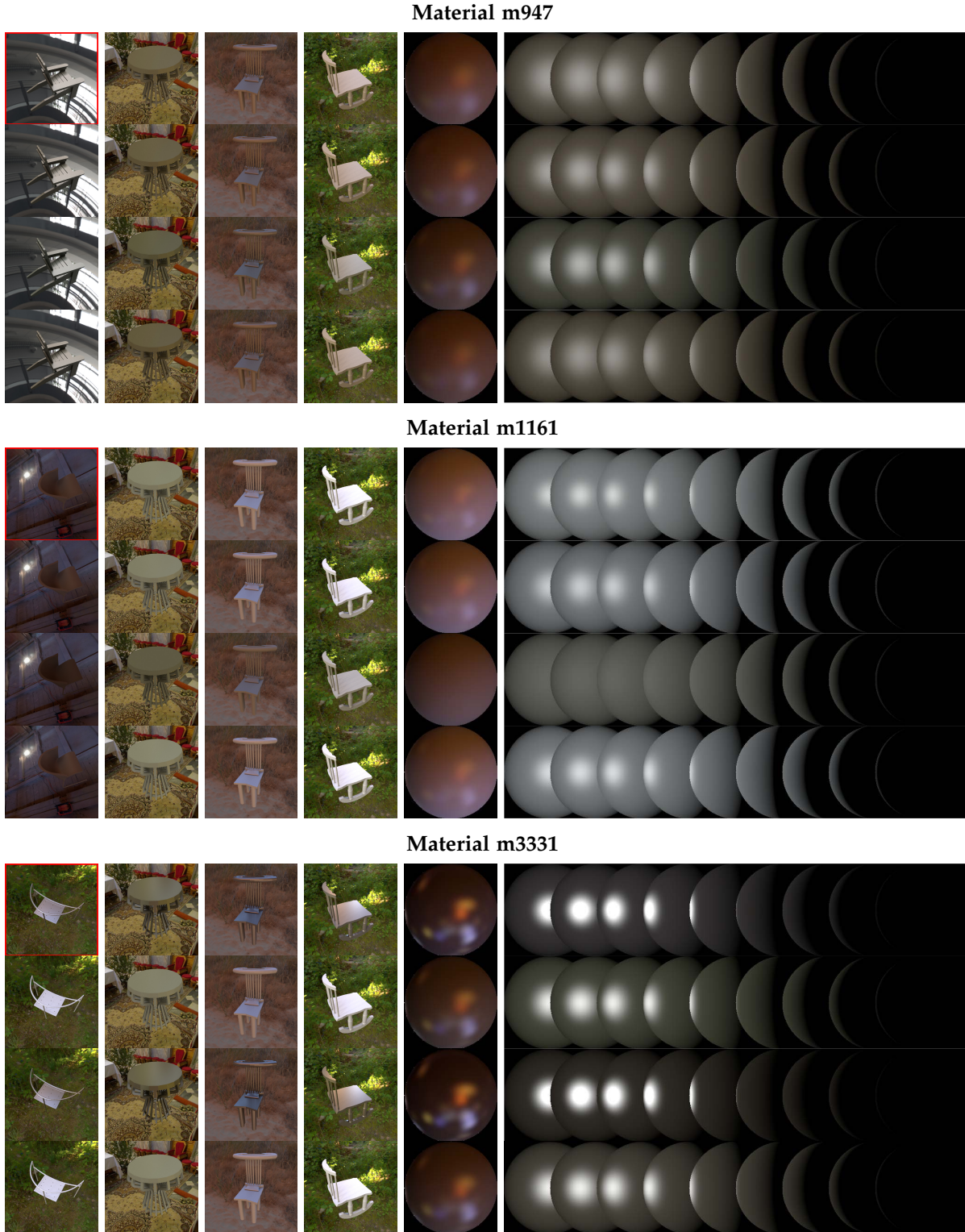


Fig. 4: Additional renderings for three randomly selected materials. For each material, images in first row are rendered from ground truth BRDF, while images in the remaining rows are rendered from BRDF estimated by one of the variations of our method: Grouplet+RMSE<sub>1</sub>+ $E_c$  (row 2), HemiCNN+RMSE<sub>2</sub> (row 3), and Grouplet+RMSE<sub>1</sub> (row 4). The ground truth image indicated with a red border is sampled from the image sequence used for inference (inputs). To demonstrate how different objects and environmental lights can change the appearance of the scene even with the same BRDF, the three images from Columns 2-4 are rendered with the same BRDF but different models and lighting. Columns 5 and 6 show a rendered sphere with the estimated BRDF and rendered spheres with varying point lighting, respectively.